A Mode-Locked Microchip Laser Optical Transmitter for Fiber Radio

Amarildo J. C. Vieira, *Member, IEEE*, Peter R. Herczfeld, *Fellow, IEEE*, Arye Rosen, *Fellow, IEEE*, Michael Ermold, *Student Member, IEEE*, Eric E. Funk, *Member, IEEE*, William D. Jemison, *Senior Member, IEEE*, and Keith J. Williams, *Member, IEEE*

***Abstract*—This paper is concerned with the optical domain generation of high-quality millimeter-wave signals for fiber-radio and other applications. The mode-locked millimeter-wave optical transmitter described here is based on simple electrooptic microchip laser technology. The transmitter can be designed to operate from a few gigahertz to 100 GHz and beyond. The residual phase noise of the laser is below −100 dBc/Hz at 1-kHz offset, which makes it well suited for optically fed millimeter-wave wireless applications. A key feature of the transmitter is its simplicity, the very small number of elements it employs and the high level of integration of the millimeter-wave and photonic components that results in a small, rugged, and reliable package. The paper describes the design, fabrication, and experimental evaluation of the transmitter.**

***Index Terms*—Fiber radio, microchip lasers, millimeter-wave generation, mode-locked lasers, optical fiber communication, optical transmitters.**

I. Introduction

GIVEN THE increasing demand for high-speed communications, there has been growing interest in developing techniques that can transmit microwave and/or millimeter-waves over optical fiber. There are both commercial and military applications for this type of technology. Commercial applications include personal communication systems (PCS) [1], and broad-band distribution of interactive multimedia services to the home [2]. Examples of military applications include Doppler radar [3] and phased array antennas [4].

The principal advantages of the transmission of high frequency signals over fiber is low attenuation and cost when compared to the conventional coaxial cable or radio transmission, and the large bandwidth even when only part of the available bandwidth is exploited. An additional advantage that makes millimeter-wave desirable for fiber radio systems is that these frequencies are highly attenuated by water molecules and oxygen in the atmosphere (i.e., 16 dB/Km at 60 GHz) [1]. This can be exploited to limit signal propagation to within the proximity of a picocell, as required for wireless secure communication and for frequency reuse.

A typical fiber radio distribution system consists of a millimeter-wave optical transmitter at the central station and numerous base stations at the picocell sites. Cost and reliability issues mandate very simple base stations with no local oscillator or sophisticated signal processing. This implies the need for an optical transmitter that can generate all the necessary optical signals as required for the generation of high-quality millimeter waves at a photodetector output located in the base station. Specifically, the detected signal at the base station must include the millimeter-wave carrier with suitable modulation for wireless transmission as described in [5].

There are many methods to achieve this, including direct modulation and mode locking of semiconductor lasers [1], [6], external modulation [7], laser heterodyning [8], and subharmonic optical injection locking [9]. However, these techniques usually lack in performance or are extremely complex and costly. In this paper, a novel optical transmitter based on a mode-locked neodymium-doped lithium niobate (Nd:$LiNbO_3$) microchip laser is described.

The mode-locked millimeter-wave optical transmitter (M-MOT) is comprised of three principal parts: the mode-locked microchip laser, an optical modulator, and a high-speed photodetctor, as depicted in Fig. 1. The mode-locked microchip laser has three components: the microchip laser which is housed in a millimeter-wave cavity, the semiconductor laser diode that "pumps" the microchip laser, and a millimeter-wave source that locks the phases of the laser longitudinal modes.

The various information signals, namely voice, video, data, and others are modulated onto a subcarrier and imposed on the optical carrier with an external optical modulator such as a Mach–Zehnder modulator. Some applications may require optical domain filtering which would also be carried out at this level. Finally, at the high-speed photodetector, the beating of the modulated locked modes yields a millimeter-wave signal with the information signals.

The approach taken in the design of the microchip laser is significantly different from past practices in two main aspects.

1) The host material for the solid-state microchip laser is an electrooptic crystal, $LiNbO_3$, which provides for efficient interaction between the optical and electric fields. This is exploited for efficient mode locking.

Manuscript received January 19, 2001; revised May 29, 2001. This work was supported by the Office of Naval Research under Grant N00014-00-1-0781 and under Grant N00014-00-1-0788.

A. J. C. Vieira is with the Broadband Communication Sector, Motorola, Horsham, PA 19044 USA.

P. R. Herczfeld, A. Rosen, and M. Ermold are with the Center for Microwave–Lightwave Engineering, Drexel University, Philadelphia, PA 19044 USA.

E. E. Funk and K. J. Williams are with the Naval Research Laboratory, Washington, DC 20375 USA.

W. D. Jemison is with the Department of Electrical and Computer Engineering, Lafayette College, Easton, PA 18042 USA.

Publisher Item Identifier S 0018-9480(01)08701-4.

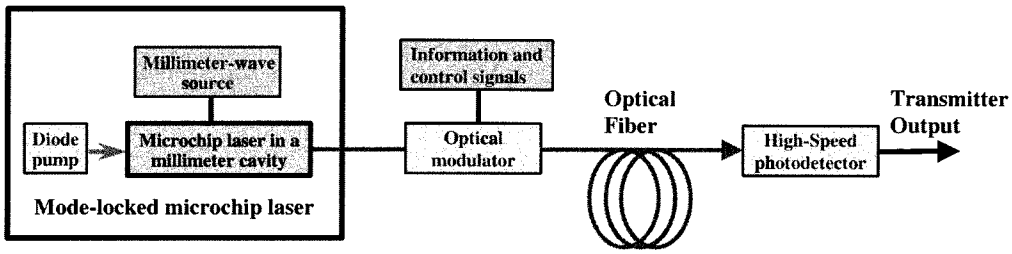

Fig. 1. Block diagram of the M-MOT.

2) The laser and the microwave components are fully integrated in a compact, rugged and low cost package, which reduces parasitic effects and therefore provides for better performance.

The following sections of the paper describe design issues as well as several stages of hardware development and performance results.

II. Mode-Locked Microchip Laser

The core of the M-MOT is the solid-state microchip laser. Microchip lasers are monolithic flat–flat optical cavities formed by a short length of gain material and dielectric mirrors deposited directly on their end facets [10]. Since the host material, lithium niobate, is electrooptic, the laser chip can be placed in a millimeter-wave cavity to facilitate effective interaction of the optical and millimeter-waves resulting in superior mode-locking performance [11]. Therefore, the motivation for using microchip lasers is driven by the following three main factors.

1) Solid-state lasers generally exhibit better stability, lower noise, and higher output power than semiconductor lasers.
2) The microchip configuration provides a low cost, compact, short length cavity, which is very suitable for mode-locking at high millimeter-wave frequencies.
3) Solid-state lasers lend themselves to integration with the microwave subsystems, yielding a low cost, rugged, integrated package that can be manufactured in large quantity.

With regard to the design of the mode-locked microchip laser emphasis was on simplicity and minimizing the number of component employed. The following specific goals were established:

1) efficient optical coupling of the semiconductor diode pump beam into the microchip laser;
2) efficient coupling of the laser output into a single-mode fiber;
3) optimal interaction between the millimeter-wave and optical fields;
4) use of low noise and low cost millimeter-wave input signal for mode locking.

A. Microchip Laser Crystal Design

The microchip laser used in this paper employs a y-cut lithium niobate ($LiNbO_3$) crystal as a host material, doped with 1-atm% of neodymium (Nd) to provide for optical gain. In addition, 5-atm% of magnesium oxide (MgO) was also added to the melt before pulling to reduce the effects of photorefractive damage [12]. Lithium niobate was selected for the laser because of its excellent optical and electrooptical properties, principally its large electrooptic coefficients. Dielectric mirrors were then directly deposited on the crystal facets, forming an optical cavity. The length of the laser cavity was 3.48 mm, which corresponds to a round-trip time of 50 ps, or an axial mode spacing of 20 GHz, matching the desired millimeter-wave subcarrier for this particular experiment. The laser cross section is 1×1 mm. It is important to note that this technique can be extended to other frequencies by properly scaling the length of the microchip laser cavity.

The immediate availability of neodymium-doped lithium niobate, which lases at 1.084 μm, represents a critical first step in development of the transmitter. Current efforts with erbium-doped lithium niobate and erbium-doped glass/lithium niobate composite crystals show promise for device development at the important 1.5-μm wavelength range.

B. Millimeter-Wave Cavity Design

In order to achieve low-noise millimeter-wave generation, the microchip laser must be mode locked to an external millimeter-wave signal. In our paper, this millimeter-wave signal is coupled to the $Nd:LiNbO_3$ microchip laser through a reentrant microwave cavity, depicted in Fig. 2(a).

The reentrant coaxial cavity was designed to match the axial mode spacing of 20 GHz. The basic design used a transmission line analysis, with the cavity modeled as a short length of lossless coaxial transmission line, terminated by the capacitance of the gap between the center conductor and the bottom of the cavity [13]. The cavity length is selected such that the transmission line inductive reactance cancels the gap's capacitive reactance at the desired resonant frequency of 20 GHz. Both the fringing capacitance of the gap [14] and the capacitance of the solid-state laser chip are included in this analysis. Thus, a first-order approximation of the required cavity length is obtained.

The mechanical design provides course frequency tuning with a cavity length adjustment about the nominal value and fine adjustment with a tuning screw in the sidewall of the cavity. The mechanical design also incorporates an alignment groove in the bottom of the cavity to facilitate the alignment of the laser chip and input and output optics. The 20-GHz mode-locking signal is coupled into the cavity by a small loop antenna (inductive coupling) located on the cavity sidewall. In addition, a temperature sensor and a thermoelectric cooler are incorporated into the microwave cavity in order to keep the cavity and the laser at a fixed temperature.

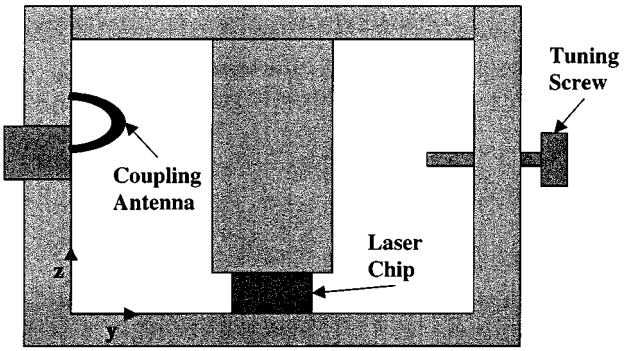

(a)

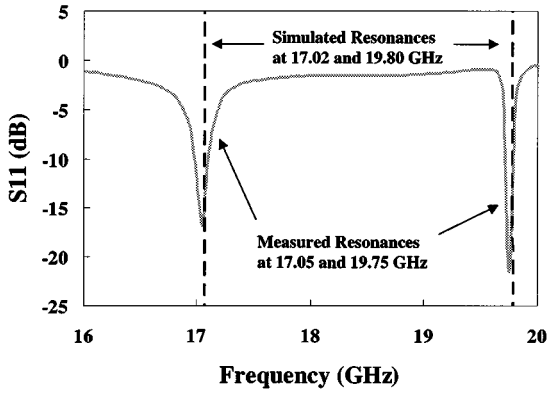

(b)

Fig. 2. (a) Cross section of the cylindrical reentrant microwave cavity with the microchip laser. (b) Measured S_{11} of the reentrant cavity with the microchip laser. Dotted lines indicate simulated resonant frequencies.

C. Mode-Locking Signal Coupling

In order to facilitate the most effective interaction between optical and millimeter-wave fields, the laser chip is placed in the center of the gap between the center conductor and the bottom of the reentrant cavity where the electric field is highest. This location will provide the strongest electrooptic interaction and should provide the best mode-locking performance. However, it should also be noted that mode-locking theory is not totally developed for the case where both the gain (for lasing) and electrooptic (for mode locking) properties are in the same medium and occupy the entire laser cavity [15]. Therefore, there is some uncertainty with respect to the field distribution required within the crystal for optimum mode locking.

In order to gain insight into the mode-locking signal coupling, a finite element computer simulation of the millimeter-wave field distribution within the laser and cavity was initiated using a commercially available high frequency structure simulator (HFSS). The reentrant cavity, solid-state laser chip, alignment groove, coupling probe, and tuning screw are all incorporated into the model. The simulated resonance frequencies of 17.02 and 19.80 GHz for this model are accurate to within 1% of the measured values determined via an S_{11} measurement, 17.05 and 19.75 GHz, respectively, as indicated in Fig. 2(b). The electric field distributions in the reentrant cavity and laser chip were also computed for the dominant mode at 19.80 GHz. The field distribution is stronger in the laser chip than in the open cavity as desired, as expected from the large dielectric constant of the laser chip (the relative dielectric constant is 26 in the z-direction at 9 GHz) [16]. The nonuniform field distribution is symmetric along the longitudinal axis of the laser chip with the highest field concentration occurring at the center of the laser and mostly concentrated along the z-axis. It is expected that a nonuniform distribution will result in the best mode coupling and, consequently, optimum mode locking [15]. The insight gained from these and ongoing simulations will ultimately lead to a complete mode locking theory for this unique laser.

D. System Integration

During the development of the M-MOT transmitter the issues outlined earlier were systematically addressed, leading to three different packaging configurations. Each generation used the same laser chip and basic reentrant cavity design. However, each successive configuration employed a higher level of integration. The three generations of laser hardware development are discussed below.

1) First Generation—Baseline Design: Our baseline proof-of-principle design [11], [17] employed our optical/microwave cavity, an external semiconductor diode pump laser, and an external microwave source. While meeting performance goals, the baseline design consisted of several external components rather than a single package. Hence, further developments were pursued.

The external semiconductor pump laser diode operated at 814 nm with an output power of 280 mW. The pump beam was coupled to the microchip laser through a fiber imbedded in a ceramic sleeve. The ceramic sleeve was aligned with the collimator and the laser placed in between them into an alignment grove designed to aid in the mechanical alignment of the semiconductor laser chip. The microchip laser output was coupled to a single-mode fiber using a fiber collimator. The mode-locking signal was obtained from an external frequency synthesizer or a Gunn oscillator.

2) Second Generation—Integrated Millimeter-Wave Source: The transmitter second generation emphasized the replacement of the external synthesizer with a compact, low-cost millimeter-wave signal source. It was found that a Gunn oscillator could easily be packaged together with the reentrant microwave cavity leading to a compact design. Furthermore, the $+10$ dBm of millimeter-wave power from the Gunn oscillator is sufficient for mode locking. We also note that efforts are currently underway to integrate the Gunn oscillator into the microchip laser housing to promote even greater size reduction. The spectra of the free-running and mode-locked signals are depicted in Fig. 3. The phase noise is adequate for many communications applications, but could be improved further by use of an equally compact lower phase-noise source such as a dielectric resonator oscillator (DRO).

3) Third Generation—Integrated Pump: The third generation of the transmitter is designed and under test. This is a more compact configuration with an internal semiconductor pump. A laser diode chip is incorporated into the reentrant microwave cavity as shown in Fig. 4. With this approach only one temperature controller is used to stabilize the pump and reentrant cavity. Once again, the pump beam and the collimator are aligned, and the laser chip is adjacent to the pump. This configuration is easier to work with and allows for systematic

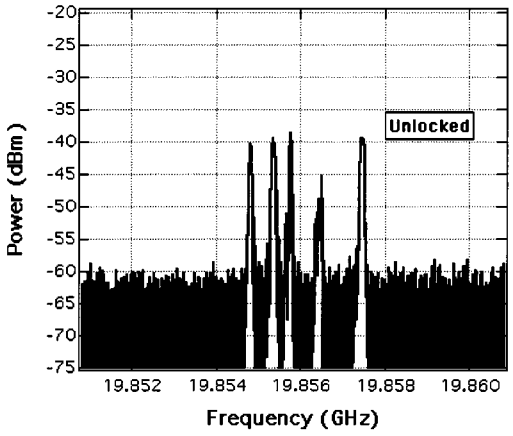

(a)

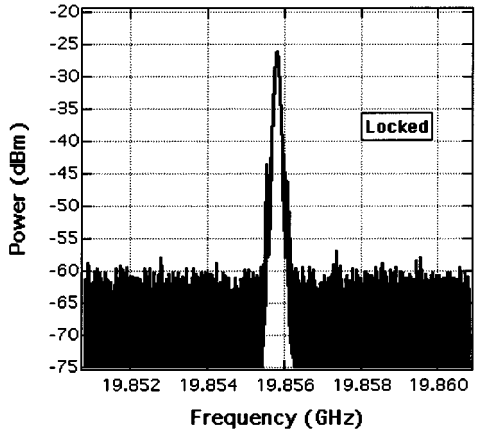

(b)

Fig. 3. Microwave spectrum of the laser output. (a) Free-running. (b) Mode-locked microchip laser.

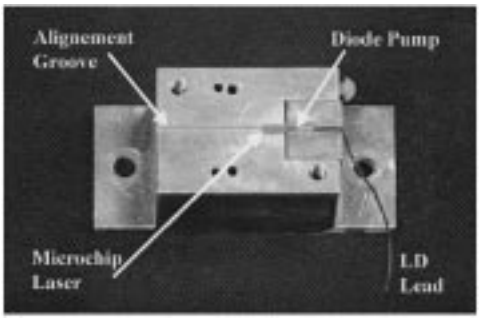

Fig. 4. Depicts the inside of the cavity, with the top removed. The pump diodes are permanently affixed and the laser chip is inserted into the grove.

repeatability. These efforts in system integration resulted in an integrated package design, consisting of a rugged cavity comprised of the laser chip, two active components, namely the diode pump and the Gunn diode each driven by single dc inputs, one temperature controller, and one optical output.

III. Experimental Characterization of the Mode-Locked Microchip Laser

A thorough characterization of the mode-locked optical transmitter requires measurements in both the optical and millimeter-wave domains. This section describes the tests performed in both of these domains.

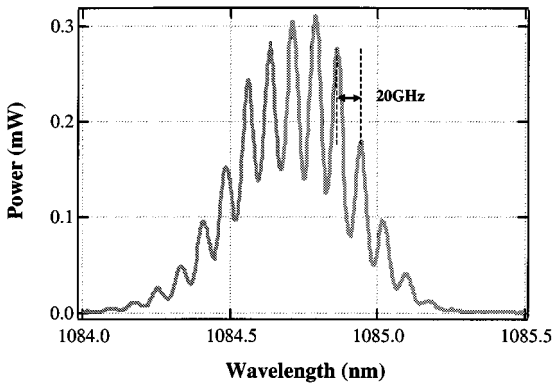

Fig. 5. Optical spectrum of the mode-locked laser output. The resolution is 0.05 nm.

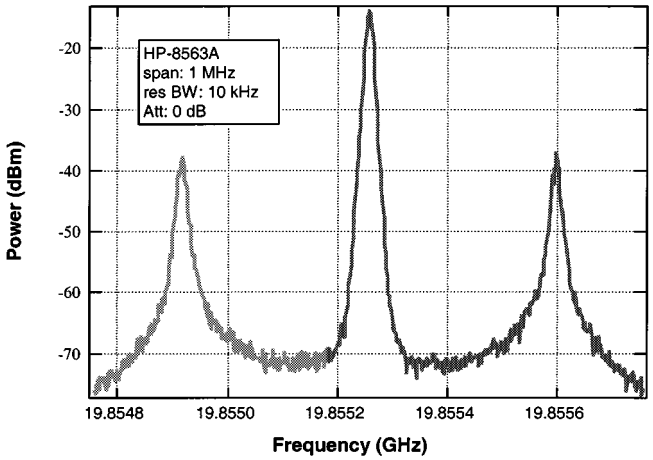

Fig. 6. Microwave spectrum of the mode-locked laser output. The frequency span and the resolution bandwidth for this measurement are 1 MHz and 10 kHz, respectively.

The 20-GHz mode-locking signal from a Gunn oscillator or a synthesizer was applied to the reentrant microwave cavity. The microwave frequency was set to correspond to the free spectral range of the laser and the microwave cavity was adjusted to resonate at this particular frequency. The mode-locked laser output was applied to an optical spectral analyzer, microwave spectrum analyzer, and a phase-noise measurement setup for the optical and microwave measurements.

A. Optical Domain Characterization

The optical spectrum of the mode-locked laser was measured using an optical spectrum analyzer with a resolution of 0.05 nm (i.e., 12.8 GHz) at 1.084 μm. The result, shown in Fig. 5, reveals stable modes spaced at 20 GHz with a well-defined Lorentzian-like distribution.

B. Millimeter-Wave Domain Characterization

The detected microwave signal, which results from the beat between adjacent cavity modes, is shown in Fig. 6. These measurements were made with a high speed InGaAs Schottky photodiode (New Focus model 1014). As expected, a stable signal at 20 GHz was observed. The -23-dBc sidebands at 350-kHz offset frequency are due to the laser relaxation oscillation. We intend to suppress these by employing feedback control to the

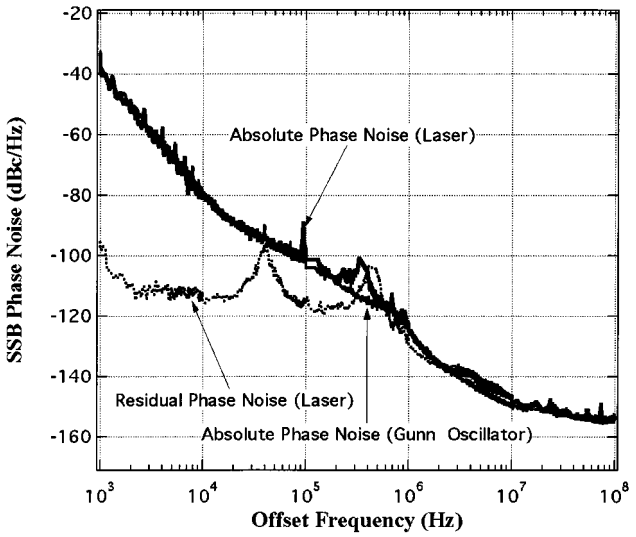

Fig. 7. Absolute single-sideband phase noise measurement for the mode-locked laser at 20 GHz. The light line is the Gunn oscillator phase noise and the darker line is after the M-MOT.

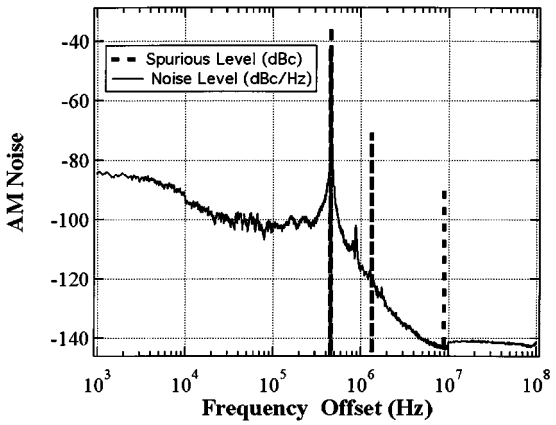

Fig. 8. RF Amplitude noise measurement (in dBc/Hz) as a function of the carrier offset frequency for the mode-locked laser at 20 GHz. The vertical lines indicate discrete spurs.

pump laser. Peak suppression of better than 30 dB has been reported in [18].

The phase and the amplitude noise of the generated 20-GHz signal were also measured. The single-sideband phase-noise measurement was performed using HP3048A measurement system. The result, shown in Fig. 7, indicates that the absolute phase noise is determined by the modulating source, the Gunn oscillator in this case. The residual phase noise was measured as well and found to be negligible over the relevant bandwidth for most applications (<-110 dBc/Hz at 10 kHz). The absolute phase noise integrated from 10 kHz to 20 MHz is -38 dBc.

The amplitude noise of the 20 GHz signal generated using the microchip laser is shown in Fig. 8. Discrete spurious signals are plotted separately from the noise power density. In contrast to the phase-noise, the laser, not the Gunn oscillator is the dominant source of amplitude noise. The -35-dBc discrete peak at 460 kHz is due to the laser relaxation oscillation. The exact frequency of this oscillation is dependent upon our alignment of the output coupler. The integrated amplitude noise (discrete spurious interference not included) from 10 kHz to 20 MHz is -27 dBc.

TABLE I
SUMMARY OF THE MICROCHIP LASER SUBSYSTEM RESULTS

Parameter	Value
Microchip laser host material	$LiNbO_3$
Microchip laser doping	Nd (1 atm. %)
Microchip laser size (for 20 GHz signal generation)	1x1x3.4 mm
Lasing wavelength	1.084 μm
Optical linewidth	<25KHz
Lasing efficiency	18%
Laser output power (average)	50 mW
Millimeter-wave frequency	20 GHz
Millimeter-wave mode locking power (threshold)	6 dBm
Modulation index	98%
linewidth of millimeter-wave signal	<80 KHz
Phase noise of millimeter-wave signal - integrated	-38dBc
Amplitude noise of millimeter-wave signal - integrated	-27dBc

System level performance tests including vector signal analysis have provided secondary verification of the noise levels measured here. Furthermore, these tests indicate that these levels are sufficient to ensure minimal impairment to QPSK modulation at a 10-Mb/s channel rate [5].

IV. SUMMARY AND CONCLUSION

A novel millimeter-wave optical transmitter was designed, fabricated, and experimentally characterized. The heart of the transmitter is a mode-locked electrooptic microchip laser whose most desirable attributes are simplicity, compactness, high level integration of the millimeter-wave and photonic components and superior performance, particularly regarding phase noise. The transmitter was conceived as part of a fiber-radio system and it meets all the requirements for this application. Table I summarizes the important characteristics of the microchip laser subsystem.

Current efforts, with promising preliminary results, are focusing on developing mode-locked lasers in Er:$LiNbO_3$ and in Er : Glass/$LiNbO_3$ composites. The erbium-doped lasers will operate at the more conventional wavelength of 1.5-μm wavelength range. A more powerful pump source and better optical coupling from the pump into the laser is expected to increase the optical output power to several hundred milliwatts. The longitudinal mode spacing of the laser can be readily extended to 100 GHz and beyond by proper scaling of the laser chip. Subharmonic mode locking would also allow a lower frequency locking source to be used. Specifically, we have successfully obtained a stable 40-GHz mode-locked component at the laser output when locked to either a 20- or 40-GHz source.

The simplicity of the mode-locked microchip laser coupled with efficient, integrated packaging of the millimeter wave and

photonic components imply high reliability and reduced cost. Although the Mach–Zehnder interferometer is not discussed here, it should be pointed out that since both the microchip laser and the modulator use $LiNbO_3$ there is a distinct possibility for their chip level integration as well. The generation and transmission of high quality millimeter-wave signals over fiber has numerous potential applications. The M-MOT device discussed in this paper was specifically designed for fiber-radio and LMDS, and it meets and exceeds the requirements for these particular applications. However, by suitable tailoring of the device, it can be adopted to other applications such as the optically fed and controlled millimeter-wave phased-array antenna and high-sampling-rate photonic analog–digital converters (ADC). Some other applications, such as pulsed Doppler radar at 94 GHz, have more stringent requirements particularly in terms of phase noise (-130 dBc/Hz or less at 100-kHz offset). Optical domain feed back can dramatically increase the Q of the millimeter-wave resonator and thus reduce noise further [19].

ACKNOWLEDGMENT

The authors would like to thank G. Mizell and G. Quarles from VLOC for growing and processing the Nd-doped lithium niobate crystals and R. Esman and P. Matthews for valuable suggestions.

REFERENCES

[1] H. Ogawa, D. Polifko, and S. Banba, "Millimeter-wave fiber optics systems for personal radio communication," *IEEE Trans. Microwave Theory Tech.*, vol. 40, pp. 2285–2293, Dec. 1992.

[2] Z. Ahmed *et al.*, "Millimeter-wave (37GHz) transmission data (up to 500Mb/s) in an optically fed wireless link incorporating a hybrid mode-locked monolithic DBR laser," in *Int. Microwave Photon. Topical Meeting*, Kyoto, Japan, 1996, pp. 45–48.

[3] E. C. Niehenke and P. Herczfeld, "An optical link for W-band transmit/receive applications," in *IEEE MTT-S Int. Microwave Symp. Dig.*, vol. 1, June 1997, p. 35.

[4] A. S. Daryoush *et al.*, "Optically controlled phased array at C-band," in *IEEE AP-S/URSI Int. Symp. Dig.*, vol. 1, July 1992, pp. 466–469.

[5] E. E. Funk, P. R. Herczfeld, W. D. Jemison, and M. Bystrom, "Performance limits of hybrid fiber/millimeter-wave wireless system," in *Int. Microwave Optoelectron. Conf.*, Aug. 6–10, 2001.

[6] D. Novak, C. Lim, and H. F. Liu, "Optimization of millimeter-wave signal generation using multi-electrode semiconductor lasers with subharmonic electrical injection," in *Int. Microwave Photon. Topical Meeting*, Kyoto, Japan, 1996, pp. 85–88.

[7] K. Noguchi, O. Mitomi, H. Miyazawa, and S. Seki, "A broad-band Ti : LiNbO3 optical modulator with a ridge structure," *J. Lightwave Technol.*, vol. 13, pp. 1164–1168, June 1995.

[8] G. J. Simonis and K. G. Purchse, "Optical generation, distribution, and control of microwaves using laser heterodyne," *IEEE Trans. Microwave Theory Tech.*, vol. 38, pp. 667–669, May 1990.

[9] A. S. Daryoush, "Optical synchronization of millimeter-wave oscillator for distributed architectures," *IEEE Trans. Microwave Theory Tech.*, vol. 38, pp. 467–476, May 1990.

[10] J. J. Zayhowski and A. Mooradian, "Single-frequency microchip Nd lasers," *Opt. Lett.*, vol. 14, no. 1, pp. 24–26, Jan. 1989.

[11] A. J. C. Vieira and P. R. Herczfeld, "Nd : $LiNbO_3$ microchip laser with 20 GHz subcarrier," in *IEEE MTT-S Int. Microwave Symp. Dig.*, Denver, CO, June 1997, pp. 229–232.

[12] D. A. Bryan, R. Gerson, and H. E. Tomaschke, "Increased optical damage resistance in Lithium Niobate," *Appl. Phys. Lett.*, vol. 44, no. 9, pp. 847–849, May 1984.

[13] K. Fujisawa, "General treatment of klystron resonant cavities," *IRE Trans. Microwave Theory Tech.*, vol. MTT-6, pp. 344–358, Oct. 1958.

[14] K. C. Gupta, R. Garg, and R. Chadha, *Computer-Aided Design of Microwave Circuits*. Norwood, MA: Artech House, 1981.

[15] S. E. Harris and O. P. McDuff, "Theory of FM laser oscillation," *IEEE J. Quantum Electron.*, vol. QE-1, pp. 245–262, Sept. 1965.

[16] Y. Omachi *et al.*, "Dielectric properties of LiNbO3 single crystals up to 9 GHz," *Jpn. J. Appl. Phys.*, vol. 6, no. 12, pp. 1467–1468, Dec. 1967.

[17] A. J. C. Vieira, P. R. Herczfeld, and V. M. Contarino, "Modelocked microchip laser with millimeter wave subcarrier," in *Int. Microwave Photon. Topical Meeting*, Schloss Hugenpoet, Germany, Sept. 1997.

[18] T. J. Kane, "Intensity noise in diode-pumped single-frequency Nd : YAG lasers and its control by electronic feedback," *IEEE Photon. Technol. Lett.*, vol. 2, pp. 244–245, Apr. 1990.

[19] X. S. Yao, L. Davis, and L. Maleki, "Coupled optoelectronic oscillators for generating both RF signal and optical pulses," *J. Lightwave Technol.*, vol. 18, pp. 73–78, Jan. 2000.

Amarildo J. C. Vieira (S'90–M'97), photograph and biography not available at time of publication.

Peter R. Herczfeld (S'66–M'67–SM'89–F'91), photograph and biography not available at time of publication.

Arye Rosen (M'77–SM'80–F'92), photograph and biography not available at time of publication.

Michael Ermold (S'98), photograph and biography not available at time of publication.

Eric E. Funk (S'94–M'95), photograph and biography not available at time of publication.

William D. Jemison (S'83–M'85–SM'96), photograph and biography not available at time of publication.

Keith J. Williams (S'86–M'89), photograph and biography not available at time of publication.